A femtosecond velocity map imaging study on *B*-band predissociation in CH_3I. I. The band origin

G. Gitzinger,[1,2] M. E. Corrales,[1] V. Loriot,[1,2] G. A. Amaral,[1] R. de Nalda,[2,a)] and L. Bañares[1,a)]

[1]*Departamento de Química Física I, Facultad de Ciencias Químicas, Universidad Complutense de Madrid, 28040 Madrid, Spain*

[2]*Instituto de Química Física Rocasolano, CSIC, C/Serrano 119, 28006 Madrid, Spain*

(Received 19 March 2010; accepted 25 May 2010; published online 18 June 2010)

A femtosecond pump-probe experiment, coupled with velocity map ion imaging, is reported on the second absorption band (*B*-band) of CH_3I. The measurements provide a detailed picture of real-time *B*-band predissociation in the band origin at 201.2 nm. Several new data are reported. (i) A value of 1.5 ± 0.1 ps has been obtained for the lifetime of the excited state, consistent within errors with the only other direct measurement of this quantity [A. P. Baronavski and J. C. Owrutsky, J. Chem. Phys. **108**, 3445 (1998)]. (ii) It has been possible to measure the angular character of the transition directly through the observation of fragments appearing early with respect to both predissociation lifetime and molecular rotation. (iii) Vibrational activity in CH_3 has been found, both in the umbrella (ν_2) and the symmetric stretch (ν_1) modes, with estimates of relative populations. All these findings constitute a challenge and a test for much-wanted high level *ab initio* and dynamics calculations in this energy region. © *2010 American Institute of Physics*.
[doi:10.1063/1.3455207]

I. INTRODUCTION

The C–I bond fission that occurs upon excitation of methyl iodide (CH_3I) in its first absorption band (or *A*-band) in the near UV is perhaps the most studied dissociation process in a polyatomic molecule. This is partly due to the fact that this process causes population inversion in the iodine atoms between the spin-orbit excited state $I^*(^2P_{1/2})$ and the ground state $I(^2P_{3/2})$, which are used as a laser medium in the iodine laser. The interest in *A*-band dissociation of CH_3I, however, goes far beyond this application, and both to experimentalists and theoreticians, it has constituted a benchmark for the study of multichannel dissociation processes in polyatomics (see, for example, Refs. 1–9).

The next absorption system in CH_3I, known as the *B*-band, has been by far much less studied. It contains transitions resulting from the excitation of a nonbonding $5p\pi$ electron of the I atom to a 6s molecular Rydberg orbital. The remaining three $5p\pi$ electrons are subject to strong spin-orbit coupling, so that, in C_{3v} symmetry, the ionic core can be in the $^2\Pi_{3/2}(^2E_{3/2})$ or the $^2\Pi_{1/2}(^2E_{1/2})$ states. These then couple (mainly *J-j*) with the Rydberg electron, and, as a result, several bound states exist. Transitions to those related with the $^2\Pi_{3/2}(^2E_{3/2})$ ionic core, from the ground $\tilde{X}$ state of the molecule, constitute the *B*-band of methyl iodide, spectrally located in the region from 195 to 205 nm. Given the selection rules (no transitions to either triplets or to states of $\Omega=2$ are allowed from the ground state[10]), the $^1\Pi_1$ state (denoted as state [2] in Ref. 11 and as R_1 in Ref. 6) dominates absorption from the ground state $\tilde{X}$, although weak features have been assigned to absorption to the $^1\Pi_2$ state,[11,12] which lies at slightly lower energies. All those transitions are of *E* character in C_{3v} symmetry, and are therefore perpendicular.

Contrary to the broad spectral character of the first absorption band in CH_3I, also known as the *A*-band, purely composed of dissociative valence levels, the *B*-band exhibits clear vibrational structure.[11–14] However, the resonances show considerable spectral broadening, indicating finite lifetimes, which are related to predissociation. Predissociation is believed to occur through surface crossing of the *B*-band state with some of the components of the dissociative *A*-band, but the details are not known. According to recent *ab initio* calculations by Alekseyev *et al.*,[6] it would be likely that the *E* symmetry states of the *B*-band would be predissociative due to their crossings with the repulsive $4E$ ($^3A_1$) state, which asymptotically yields $I^*(^2P_{1/2})+CH_3$. Vaida *et al.*[15] reported that more than one dissociative state should be responsible for *B*-band state dissociation, but this idea was supported by the notion that the $I^*(^2P_{1/2})$ yield was less than unity, which was later shown to be false.[16] High level, multidimensional *ab initio* surfaces of *A*-band and *B*-band states would be needed to clarify this issue.

As suggested by the previous paragraphs, many issues related to *B*-band dissociation of CH_3I are largely unknown. Although the first pump-probe measurements of the lifetime of higher-lying Rydberg states of CH_3I had been reported by Zewail and co-workers[17,18] in the early 1990s, the only direct measurements of parent lifetime in the *B*-band were obtained by Baronavski and Owrutsky in Ref. 19 and later by the same authors in Ref. 11, where a predissociation time of 1.38 ± 0.14 ps for the 0_0^0 origin band was reported. Previous

a)Authors to whom correspondence should be addressed. Electronic addresses: r.nalda@iqfr.csic.es and lbanares@quim.ucm.es.

reports[20,21] had been based on frequency-domain measurements. In particular, data based on bandwidths can only provide lower limits for the lifetime, since several spectral broadening mechanisms can participate. Even the nature of the dissociation products is still not completely clear: the $I^*(^2P_{1/2})/I(^2P_{3/2})$ yield has been the subject of controversy until recently,[16] and only very partial information has been reported on vibrational activity on the nascent CH_3 fragment.[22,23] Additionally, the angular nature of the $\tilde{X}$-$\tilde{B}$ transition has only been measured indirectly[16,22] and in non-time-resolved schemes, where loss of information due to rotation occurred. On the theory side, despite some progress made by Vaida *et al.*[15] and Alekseyev *et al.*,[6] high level *ab initio* calculations of these states, together with the couplings to *A*-band states, are still lacking.

Femtosecond laser pump-probe schemes, coupled with charged particle imaging detection, have revealed themselves as powerful tools to unravel the details of fast dissociation processes,[24–32] in particular when state-selective versus nonselective ionization schemes are employed. In this work, we have studied the dissociation of CH_3I after one-photon absorption to the origin of the *B*-band at 201.2 nm. This has been followed by either probing the decay of the parent CH_3I, or measuring appearance times of the I and CH_3 fragments through either resonance-enhanced multiphoton ionization (REMPI) or multiphoton ionization (MPI). This methodology has allowed us to unambiguously measure the $I^*(^2P_{1/2})$ yield, the anisotropy of the transition at early times (i.e., before rotation plays a role), the lifetime of the vibrationless component of the *B*-band state, and the propagating time of the wave packet along the dissociative state (from the difference in initial time of the parent and fragment measurements). Additionally, comparison of state-selective versus nonselective ionization of CH_3 has allowed us to quantify yields for excitation of several vibrational states in the nascent fragment.

II. EXPERIMENTAL

The laser, an amplified Spectra Physics Ti:sapphire system, delivers 3.5 mJ pulses of 50 fs duration centered around 805 nm at 1 kHz repetition rate. The main beam is split into two arms, one of which is used to pump an optical parametric amplifier tuned to generate signal pulses in the 1.2–1.3 μm region, which are later frequency quadrupled to either around 305 nm for 2+1 REMPI probing of I atoms, or around 330 nm for 2+1 REMPI probing of the CH_3 fragments. Probe pulse energies are typically around 3 μJ. The other fundamental 805 nm arm is frequency quadrupled in a device consisting of a tripling unit followed by a sum-frequency mixing unit between the third harmonic and the fundamental. This arm provides radiation resonant with the 0_0^0 vibronic transition of the *B*-band in CH_3I around 201.2 nm with a full width at half maximum (FWHM) bandwidth of 1 nm, with typical pulse energies of <1 μJ. The polarization of both pump and probe beams is horizontal, and their geometries on target are controlled through the use of telescopes. The temporal delay between the pulses is controlled by a motorized delay stage placed in the probe arm, with a resolution of $\approx$1 fs. Pump and probe beams are propagated collinearly and focused with a 25 cm focal length lens. In some experiments, a nonresonant probe laser at the fundamental 805 nm frequency, of around 15 μJ/pulse, was used instead of the UV probe. The instrument temporal response time, considered as the temporal cross-correlation of the pump and probe beams, was measured through MPI of Xe, obtaining a value of $\approx$400 fs. This also served to determine the zero of time in part of the experiments.

CH_3I, kept at a temperature of 0 °C, is seeded in Ar, at a typical total pressure of 2.5 bar, and expanded into vacuum through a 0.5 mm nozzle diameter, 1 kHz homemade piezoelectric pulsed valve. The molecular beam passes through a 1 mm skimmer that separates the source chamber from the ionization chamber. Working on the earliest part of the gas pulse allowed us to avoid clustering conditions in the beam.

Ions formed in the interaction region are extracted perpendicularly by a set of open-lens electrodes that constitute an ion lens system working in velocity mapping configuration[33] ensuring 100% transmittance and a one-to-one mapping of velocity vectors onto points on the detector plane. At the end of a 50 cm time-of-flight tube sits the detector, a dual microchannel plate (MCP) in Chevron configuration, coupled to a phosphor screen. Typical repeller voltages were 5200 V, with optimum velocity mapping conditions found for $V_{\text{extractor}}/V_{\text{repeller}}=0.76$. Mass selection was achieved through gating the gain in the front MCP plate. The images thus generated on the phosphor screen are recorded with a Peltier-cooled 12 bit charge coupled device camera. Typical acquisition times for each image are 30 s, corresponding to 30,000 laser shots. The calibration of the apparatus was done by measuring the CH_3^+ image upon 268 nm photodissociation of CH_3I and resonant $CH_3(\nu=0)$ ionization, and using the known kinetic energy (KE) release of the $CH_3(\nu=0)+I^*(^2P_{1/2})$ and $CH_3(\nu=0)+I(^2P_{3/2})$ channels.[27,33] The best energy resolution obtained corresponds to $\approx$100 meV in the 2.5 eV region.

The methodology for the acquisition of delay scans was as follows. Once the proper wavelengths were chosen and the geometry on target optimized, including spatial pump-probe overlap, sets of images were acquired and personal computer stored as the temporal delay was scanned across the desired range. An experimental run consisted of a repeated sequence (typically 20) of such scans, and final stored images corresponded to the accumulation of the complete sequence. This procedure proved very effective in the optimization of signal-to-noise ratio. Images were Abel inverted using the pBASEX method.[34]

Some of the mass-selected images showed several contributions, corresponding to more than one formation channel. In these cases, a multidimensional three-dimensional (radius, angle, time) software made in-house[35] was employed to fit the images as a sum of contributions characterized by the product of a radial, an angular and a temporal function with adjustable parameters. This method allowed us to study the desired contribution isolated from other contributions that sometimes overlap partially.

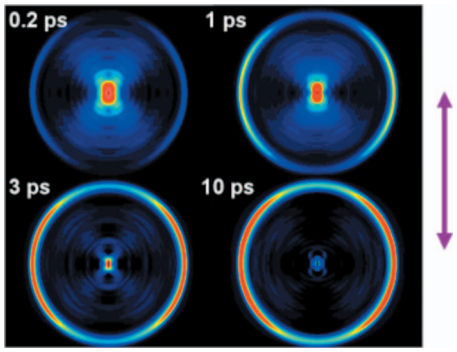

FIG. 1. Sequence of Abel-inverted iodine images, in false color, as a function of pump-probe delay time for a pump laser center wavelength of 201.2 nm (origin of *B*-band) and a probe laser center wavelength of 304.5 nm. The ring corresponds to the $I^*(^2P_{1/2})+CH_3$ channel. The double-sided arrow indicates the polarization axis of both lasers.

III. RESULTS AND DISCUSSION

The absorption spectrum of CH_3I in the 200 nm region shows discrete peaks corresponding to vibronic transitions[11–13] that are lifetime broadened. By using a short pump pulse centered at 201.2 nm (FWHM=1 nm), only the band origin 0_0^0 is expected to be excited. This is the strongest feature in the absorption spectrum and the closest resonance, a weak line assigned to the $[1]6_0^1$ transition, lies at 199.8 nm, beyond the bandwidth of the pump laser.

Nascent products appearing after short-pulse 201.2 nm excitation to the band origin of the *B*-band were measured through femtosecond REMPI or MPI. For detection of the iodine atom, 2+1 REMPI schemes exist in the 305 nm region both for $I(^2P_{3/2})$ and $I^*(^2P_{1/2})$.[36] It is an objective of this work to clearly establish the nature of the dissociation channels that are open in CH_3I upon *B*-band excitation, since some ambiguities persisted in the literature on the $I(^2P_{3/2})$ versus $I^*(^2P_{1/2})$ yield, as will be discussed later.

A previous *A*-band excitation experiment was performed, carried out at 268 nm, where it is known that both $I(^2P_{3/2})$ and $I^*(^2P_{1/2})$ are produced. This was used as a test of the sensitivity to $I(^2P_{3/2})$ and $I^*(^2P_{1/2})$. The conclusion of such study was that, given the bandwidth of the probe laser, at a center wavelength of 306.5 nm, the system is only sensitive to the presence of $I^*(^2P_{1/2})$ (through the intermediate states $6p\ ^4P_{3/2}$ and $6p\ ^3D_{3/2}$). However, at a center wavelength of 304.5 nm, both $I(^2P_{3/2})$ (through the $6p\ ^4D_{7/2}$ and $6p\ ^4D_{1/2}$ states) and $I^*(^2P_{1/2})$ (through the $6p\ ^4P_{3/2}$ and $6p\ ^4D_{1/2}$ states) can be simultaneously detected resonantly. Under 304.5 nm center wavelength probing, therefore, it was checked that the I and I^* channels of *A*-band dissociation of CH_3I appear as distinct rings in the image.

The same 2+1 REMPI schemes were applied to iodine atom production in *B*-band dissociation at 304.5 and 306.5 nm center wavelengths of the probe beam. The main result of this experiment was that only one ring is present, regardless of the probing wavelength (see Fig. 1). This constitutes proof that $I^*(^2P_{1/2})$ is the only product of this dissociation. This result is interesting, since there has been some controversy over this issue. Leone *et al.*[37] reported a $I^*(^2P_{1/2})$ yield of 0.70 ± 0.04. Very recently, Taylor *et al.*[16] reported the agreement with this value when the diode laser gain/absorption method (the same employed in Ref. 37) was used. However, Taylor *et al.* noted that a systematic error is associated with this technique. They claimed that, by using Doppler-resolved frequency-modulated (FM) absorption spectroscopy, they measured a quantum yield of unity for $I^*(^2P_{1/2})$. This is also in agreement with the measurements by de Vries *et al.*,[22] who claimed that only $I^*(^2P_{1/2})$ was observable, and with calculations[15] that indicate that the surface(s) of the *A*-band system of CH_3I that are responsible for *B*-band predissociation correlate with the formation of $I^*(^2P_{1/2})+CH_3$. Our experimental results neatly show that this is indeed the case.

Delay scans where iodine atom images were acquired as a function of the temporal separation between the pump and probe lasers were performed in the temporal range of −1 to 20 ps with variable steps from 75 to 500 fs. Some examples extracted from a typical sequence of Abel-inverted images can be seen in Fig. 1. In this case, 2+1 REMPI probing of I was carried out at a center wavelength of 304.5 nm. In the images of Fig. 1 corresponding to short delay times between the pump and probe beams (mainly 0.2 and 1 ps), it is possible to see a contribution in the center of the image, corresponding to relatively low kinetic energies. We believe this contribution to be caused by ion dissociation after multiphoton absorption processes. This is supported by the fact that this component remains unaltered through tuning the probe laser wavelength off-resonance of the iodine 2+1 REMPI transition. It may carry information on *B*-state dynamics through the decay of the parent, but its interpretation is likely to be complicated by dynamics on the ionic surfaces. The only neat contribution corresponding to *B*-band excitation is the large ring whose intensity grows as the temporal delay increases, until it stabilizes for delay times of >6 ps. This ring corresponds to the $I^*(^2P_{1/2})+CH_3$ channel, where the $I^*(^2P_{1/2})$ peak is significantly broad, due to the contribution of several vibrational states of the CH_3 cofragment, which give rise to a distribution of available kinetic energies. The vibrational activity of CH_3 will be discussed later.

From angular integration of the Abel-inverted images, the KE distribution of the iodine atom can be obtained. This is shown in Fig. 2(a) for a delay time between the pump and probe lasers of 15 ps. The maximum available KE that could be acquired by the iodine atom in the $I^*(^2P_{1/2})+CH_3$ channel can be calculated through $KE_{max}(I)=(m_{CH_3}/m_{CH_3I})\times(h\nu_{201.2\ nm}-D_0-E_{SO})$, where m_i is the mass of the species i, $h\nu$ is the photon energy, D_0 is the dissociation energy of the C–I bond in CH_3I, and E_{SO} is the spin-orbit energy split in iodine. This calculation yields a value of $KE_{max}=0.297$ eV. This value has been indicated in Fig. 2(a) with a red vertical line. The observation of a tail in the KE distribution toward larger energies can be partially explained by the finite resolution of the apparatus, although there may be some degree of rotational excitation in the parent that shows as a slightly higher available KE. On the other hand, if some excitation is present in CH_3 (vibrational and rotational), the maximum KE for I is reduced. An indication of the maximum KE expected for the iodine atom for some vibrational combinations in CH_3 is given in the figure. From the asym-

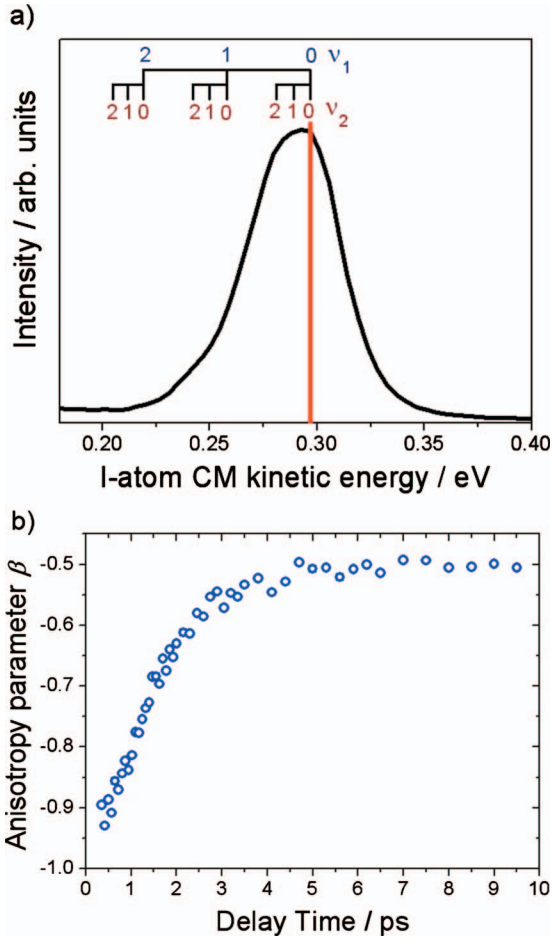

FIG. 2. (a) Center-of-mass KE distribution of the iodine atom for a delay time of 15 ps between the pump (201.2 nm) and probe (304.5 nm) lasers. The red vertical line shows the maximum available energy that could be acquired by iodine in the $I^*(^2P_{1/2})+CH_3(\nu=0)$ channel (see text). The maximum available energy corresponding to some channels where the CH_3 fragment is vibrationally excited is also indicated in the figure. (b) Angular distribution of $I^*(^2P_{1/2})$ fragments with respect to the laser polarization direction as a function of time. Open circles show the anisotropy parameter β as a function of delay time between pump and probe lasers (see text).

metric shape of the I peak, it is clear that some degree of vibrational excitation is present in the CH_3 cofragment.

The angular character of the measurements presented in Fig. 1 will now be undertaken. All images in Fig. 1 show perpendicular character, i.e., concentration of iodine ions in the region of the equator of the sphere (where the poles are defined by the polarization axis of the laser). However, the degree of anisotropy changes with time. Figure 2(b) shows the anisotropy parameter β derived from a fit to the equation $I(\theta)=(\sigma/4\pi)[1+\beta P_2(\cos\theta)]$ (Ref. 38) as a function of time, where σ is the total absorption cross section, θ is the angle between the polarization axis of the photolysis laser and the fragment velocity vector, and $P_2(\cos\theta)$ is the second Legendre polynomial. As is clear in the figure, in the early time region $\beta=-1$, as is characteristic of a purely perpendicular transition. For longer delay times, and indeed for asymptotic delays, the initial anisotropy is noticeably diminished to final values of $\beta=-0.50\pm0.07$. Estimates of the expected loss of anisotropy upon molecular rotation can be obtained using the semiclassical models in Refs. 39 and 40. For an estimated temperature of the excited molecular sample of 40 K, a calculated asymptotic anisotropy of -0.4 is obtained. This value is slightly above the experimental result of -0.5, but compatible given the experimental error and the uncertainty over the temperature value.

That the $\tilde{X}$-$\tilde{B}$ transition in CH_3I is of perpendicular character had been known for a long time,[10] but the only direct measurement of product angular distributions that has been found in the literature was carried out by Van Veen *et al.*[22] at 193.3 nm using photofragment translational spectroscopy. They reported a value of $\beta=-0.72\pm0.10$. Very recently, Taylor *et al.*[16] gave a value of $\beta=-0.71\pm0.09$ obtained through Doppler-resolved FM absorption spectroscopy at 193.3 nm. Both explored the 2_0^2 transition, not the 0_0^0 origin, but, more importantly, both were asymptotic measurements, that is, they corresponded to probes having a response of much longer time duration than the predissociation time in the B-band ($\approx$1 ps). This was realized in both cases, and the fact that a value lower than $\beta=-1$ (expected from a perpendicular transition) was found was attributed to rotation of the molecule prior to dissociation. The time-resolved measurement of β presented in this work is a confirmation both of the purely perpendicular nature of the transition and of the important loss of anisotropy due to rotation during the excited state lifetime.

A description of the findings in the time domain will be given below. In principle, it is possible to directly measure B-band lifetimes either through the decay in the ionization of the parent molecule, detected through a REMPI process[11] or, alternatively, through the measurement of the appearance times of the resulting fragments. It is important to note that, when REMPI fragment detection is used, an additional delay time is expected to appear, due to the additional time required for wave packet dynamics on the dissociative state from the Franck–Condon region until it reaches the optical window region, near the asymptote, where resonant probing is performed. As a result, the shape of the fragment curve should be identical, only with opposite sign, and with a temporal shift, to the decay of the parent. Lifetimes can equally be extracted from the two types of measurements.

Both parent decay and I fragment appearance times were measured by acquiring collections of mass-selected images as a function of delay time between the pump and probe beams. In both cases, a 201.2 nm laser was used as pump, and a 304.5 nm laser was used as probe. Ionization of the parent CH_3I, therefore, was produced with a $1+1'$ REMPI scheme, whereas ionization of the I atoms resulting from dissociation was done with a 2+1 REMPI scheme at 304.5 nm. In the case of the parent, the signal is concentrated in the center of the image and is entirely integrated to obtain a transient. In the case of iodine, the contribution corresponding to the ring in Fig. 1 is isolated through the use of the multidimensional fitting software described previously. The results can be seen in Fig. 3. The figure shows the result of subtracting the fit of all other contributions (background) from the experimental images, and integrating the resulting image.

We have performed the analysis of the transients independently for CH_3I and I. In the case of the parent, the tran-

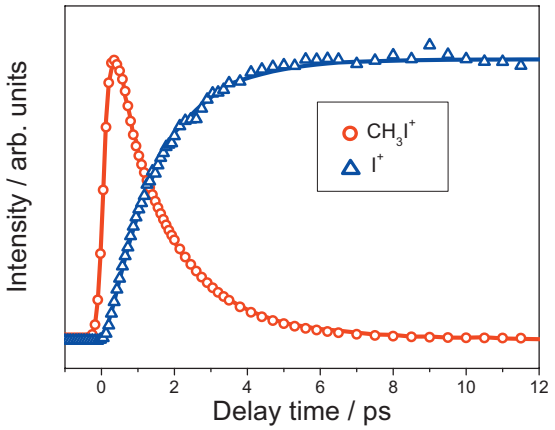

FIG. 3. Experimental transients corresponding to parent CH_3I decay (red) and iodine atom appearance (blue) after 201.2 nm *B*-band excitation of CH_3I. Probe center wavelength was 304.5 nm, exploiting the 2+1 REMPI transition for $I^*(^2P_{1/2})$ and providing sufficient energy to ionize CH_3I from the *B*-band state in a single-photon process. The time constant obtained for the lifetime of the excited state is $\tau=1.5\pm0.1$ ps (see text).

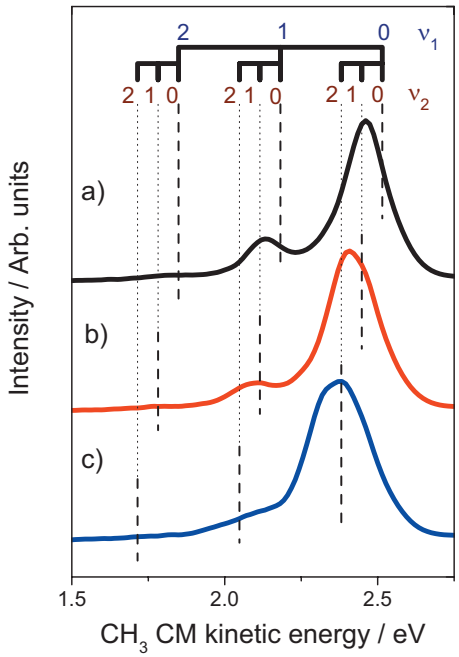

FIG. 4. CM CH_3 KE distributions. They are extracted from Abel-inverted CH_3^+ images recorded upon *B*-band excitation of CH_3I at 201.2 nm (0_0^0 band) and subsequent CH_3 2+1 REMPI probing with pulses delayed by 15 ps and spectrally centered at (a) 333.5, (b) 329.4, and (c) 325.8 nm in resonance with the *Q* branch of the two-photon $3p_z(^2A_2''\leftarrow{}^2A_2'')$ resonance in CH_3 in its 0_0^0, 2_1^1, or 2_2^2 bands, respectively.

sient was fit by the sum of a Gaussian (accounting for possible multiphoton processes in the region of temporal pump-probe overlap) and an exponential decay, in convolution with an instrument response function. This instrument response is equivalent to the cross-correlation of the pump and probe pulses, and best fits were obtained for width values of ≈400 fs. The main quantity obtained from these measurements, i.e., the decay time of the exponential, was found to be 1.5 ± 0.1 ps. For iodine appearance times, the value obtained from the multidimensional fit was 1.52 ± 0.13. Clearly the two values are compatible, and they are also compatible with Baronavski and Owrutsky's measurement of 1.38 ± 0.14,[11] although they lie in the higher part of their error bar.

As was noted before, a delay between the decay of the CH_3I parent and the appearance of the iodine atom was expected due to the wave packet motion required on the dissociative state until the asymptotic region is reached. However, considerable dispersion was found for this quantity, with a mean value of $\Delta t_0=60\pm120$ fs. We cannot therefore provide a precise clocking measurement for the bond fission process on the *A*-band surface.

A direct exploration of vibrational activity in the CH_3 fragment originating from excitation of the *B*-band of CH_3I was also undertaken. In a 1985 experiment, de Vries *et al.*[22] reported a distribution of internal energy states that was attributed to a bimodal distribution on the ν_2 umbrella mode of CH_3 after 193 nm excitation (to the 2_0^2 band of CH_3I). This was later reassigned to significant ν_1 symmetric stretch excitation in CH_3 born in the dissociation process.[23] No previous data on vibrational distribution of nascent CH_3 from the vibrationless $\nu=0$ state of the Rydberg system have been found.

A 2+1 REMPI scheme for CH_3 exists in the vicinity of 330 nm that exploits the two-photon $3p_z(^2A_2''\leftarrow{}^2A_2'')$ resonance. All ν_1, ν_3, and ν_4 modes of CH_3 have very similar values for the ground and the $3p_z$ state, producing shifts of the 0_0^0, 1_1^1, 3_1^1, and 4_1^1 bands that are within the short laser pulse spectral bandwidth. Therefore, all those transitions can in principle be observed simultaneously. The ν_2 umbrella mode, however, is only 607 cm^{-1} in the ground state, compared with 1323 cm^{-1} in the upper $3p_z$ state. This difference is beyond the laser bandwidth, and therefore, probing CH_3 vibrational activity resonantly on ν_2 requires tuning the central wavelength. In practice, this was done by using 333.5, 329.4, or 325.8 nm pulses, in resonance with the *Q* branch of the two-photon $3p_z(^2A_2''\leftarrow{}^2A_2'')$ resonance in CH_3 in its 0_0^0, 2_1^1, or 2_2^2 bands, respectively.[2] The CH_3 center-of-mass (CM) KE distributions obtained from the Abel-inverted CH_3 images acquired for each of these conditions, for a pump-probe delay time ($\Delta t=10$ ps), much longer than the dissociation time (asymptotic limit), are shown in Fig. 4.

All CH_3^+ images (not shown) show a predominant ring, and one or more lower-intensity rings at smaller radii, corresponding to the main peak and the weaker peaks at lower values of KE in Fig. 4. The main peak lies in the 2.5 eV region, and can be unambiguously assigned to methyl formed in the channel $CH_3(\nu_2)+I^*(^2P_{1/2})$ with $\nu_2=0,1,2$. The observed increasing width of the peaks for increasing vibrational state is likely to be due to rotational excitation. No evidence for a KE release in methyl compatible with the formation of the $CH_3(\nu)+I(^2P_{3/2})$ channel was found, which is an additional confirmation that the $I^*(^2P_{1/2})$ quantum yield in *B*-band dissociation of CH_3I is unity (see above). The measurements shown in Fig. 4 constitute direct proof of vibrational activity in the umbrella mode of the nascent CH_3 product upon *B*-band dissociation.

A clear second peak, with lower KE release, is visible for all probe wavelengths, becoming less clear for $\lambda_{probe}=325.8$ nm [Fig. 4(c)]. The position of this peak would be compatible with excitation in either the symmetric stretch

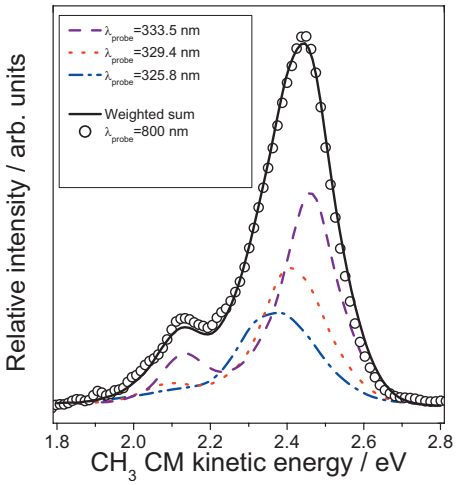

FIG. 5. CM CH_3 KE distributions obtained from Abel-inverted CH_3^+ images recorded upon *B*-band excitation of CH_3I at 201.2 nm (0_0^0 band). CH_3 MPI probing was performed with pulses delayed by 10 ps centered at 805 nm (open circles), 333.5 nm (dashed purple line), 329.4 nm (dotted red line), and 325.8 nm (dot-dashed blue line). The solid black line is the distribution obtained through the weighted sum of the KE distributions for resonant $\nu_2=0$, 1, and 2 shown in Fig. 4. The weights were optimized for best fit and are shown in Table I. They can be interpreted as relative $\nu_2=0:\nu_2=1:\nu_2=2$ populations (see text).

mode (ν_1) or the ν_3 mode, both of which have quanta of the order of 3000 cm^{-1}. It is clear that no activity in the ν_4 mode ($\approx$1400 cm^{-1}) is present. Even though assignment to either ν_1 or ν_3 would be possible, we believe that, similar to *A*-band dissociation, the axial modes would be more prone to excitation than the transverse modes. For the data taken at 333.5 nm, therefore, we ascribe this channel to $CH_3(\nu_1=2)+I^*(^2P_{1/2})$. In this case, another weaker contribution, which can be assigned to $CH_3(\nu_1=2)+I^*(^2P_{1/2})$, can be barely observed. For the images taken at 329.4 nm, peaks that can be assigned to $CH_3(\nu_1=1,\ \nu_2=1)+I^*(^2P_{1/2})$ and $CH_3(\nu_1=2,\ \nu_2=1)+I^*(^2P_{1/2})$ can be observed. At 325.8 nm probe wavelength, the signal drops significantly and only one weak contribution is clearly detected, which we believe reveals CH_3 formation in the $CH_3(\nu_1=1,\ \nu_2=2)+I^*(^2P_{1/2})$ channel.

Therefore, this is the first time that evidence for activity in the ν_1 and ν_2 modes (as well as combinations of those) of CH_3 born after *B*-band origin predissociation of CH_3I is presented. Temporally, appearance times measured for CH_3, in all vibrational states, were compatible with the value of 1.5 ± 0.1 measured for the parent CH_3I lifetime.

In order to obtain quantitative estimates of the degree of vibrational activity in nascent CH_3, ion images of this fragment were also acquired by probing with a short, nonresonant laser pulse centered at 805 nm to produce MPI. The corresponding images showed a similar overall structure, except broadened in energy, as is expected from the lack of selectivity of the vibrational state of the product fragment.

The CM KE distribution for CH_3 observed for a delay time of 10 ps between the 201.2 nm pump and the nonresonant 805 nm probe is shown in Fig. 5 (open circles). Assuming that the ionization probability is practically independent on the CH_3 vibrational state in the explored range, from the comparison of the nonresonant result and the REMPI results

TABLE I. Vibrational states observed in CH_3 appearing upon *B*-band dissociation of CH_3I with estimated relative populations (see text).

ν_2	ν_1	Relative population ($\pm$10%)
0	0	37
0	1	7
0	2	$<$1
1	0	28
1	1	4
1	2	$<$1
2	0	24
2	1	$<$1

shown in Fig. 4, we can obtain an estimate of the relative vibrational populations of CH_3 over ν_2. We have therefore assumed that the nonresonant image corresponds to a superposition of the three REMPI images, with adequate weights that provide the information on relative populations. The method has consisted of finding the best fit to the nonresonant KE distribution curve by optimization of the weights (i.e., multiplicative factors). The curve obtained from this procedure is shown for comparison in Fig. 5 (black line), together with the individual contributions (colored lines). The excellent agreement found between the experimental result and this fit constitutes proof that the assumption is correct, i.e., that most of the vibrational activity is concentrated on the umbrella mode, mainly in its three lower quanta, and in part in the symmetric stretch mode ν_1. Table I shows the CH_3 vibrational states that have been detected, together with estimates of relative populations obtained through this method. Note that a good agreement is found not only for the ν_2 excitation but also for the peaks corresponding to activity on the ν_1 mode. Vibrational activity with a relatively hot distribution on the ν_2 umbrella mode of CH_3 is a consequence of the geometric change (tetrahedral to planar) occurring in CH_3 upon the C–I bond rupture in the CH_3I molecule.

IV. CONCLUSIONS

A femtosecond pump-probe experiment carried out with the velocity map ion imaging technique has been employed to obtain a detailed picture of real-time *B*-band dissociation in CH_3I. Separate resonant I and CH_3 measurements, together with nonresonant CH_3 probing, have demonstrated that the main channels that are open upon excitation in the band origin are $I^*(^2P_{1/2})+CH_3(\nu_1=0,1;\ \nu_2=0,1,2)$. Measurements of the appearance times of all products are compatible within experimental error, thus adding further proof of their common origin, and provide a value of 1.5 ± 0.1 ps for the lifetime of the vibrationless state of the *B* system. Finally, the angular (perpendicular) character of the transition has been determined through real-time detection of the anisotropy observed in the iodine images.

ACKNOWLEDGMENTS

We thank Dr. Alberto García-Vela and Dr. Jesús González Vázquez for fruitful discussions. M.E.C. acknowledges financial support from MICINN (Spain) through a FPU fellowship. This work has been financed by the Spanish

MICINN through Grant No. CTQ2008-02578/BQU, the Consolider program "Science and Applications of Ultrafast Ultraintense Lasers," Grant No. CSD2007-00013, and by the European Union ITN network "Ultrafast control of quantum systems by strong laser fields—FASTQUAST" (Grant No. PITN-GA-2008-214962). This research has been performed within the Unidad Asociada "Química Física Molecular" between Departamento de Química Física of UCM and CSIC. The facilities provided by the Centro de Asistencia a la Investigación de Espectroscopia Multifotónica y de Femtosegundo (UCM) are gratefully acknowledged.

[1] A. Gedanken and M. D. Rowe, Chem. Phys. Lett. **34**, 39 (1975).
[2] R. O. Loo, H.-P. Haerri, G. E. Hall, and P. L. Houston, J. Chem. Phys. **90**, 4222 (1989).
[3] Y. Amatatsu, S. Yabushita, and K. Morokuma, J. Chem. Phys. **104**, 9783 (1996).
[4] A. T. J. B. Eppink and D. H. Parker, J. Chem. Phys. **110**, 832 (1999).
[5] D. Xie, H. Guo, Y. Amatatsu, and R. Kosloff, J. Phys. Chem. A **104**, 1009 (2000).
[6] A. B. Alekseyev, H.-P. Liebermann, R. J. Buenker, and S. N. Yurchenko, J. Chem. Phys. **126**, 234102 (2007).
[7] D. W. Chandler and P. L. Houston, J. Chem. Phys. **87**, 1445 (1987).
[8] D. W. Chandler, J. W. Thoman, Jr., M. H. M. Janssen, and D. H. Parker, Chem. Phys. Lett. **156**, 151 (1989).
[9] D. W. Chandler, M. H. M. Janssen, S. Stolte, R. N. Strickland, J. W. Thoman, Jr., and D. H. Parker, J. Phys. Chem. **94**, 4839 (1990).
[10] R. S. Mulliken and E. Teller, Phys. Rev. **61**, 283 (1942).
[11] A. P. Baronavski and J. C. Owrutsky, J. Chem. Phys. **108**, 3445 (1998).
[12] M. R. Dobber, W. J. Buma, and C. A. de Lange, J. Chem. Phys. **99**, 836 (1993).
[13] S. Felps, P. Hochmann, P. Brint, and S. P. McGlynn, J. Mol. Spectrosc. **59**, 355 (1976).
[14] D. J. Donaldson, V. Vaida, and R. Naaman, J. Chem. Phys. **87**, 2522 (1987).
[15] D. J. Donaldson, M. S. Child, and V. Vaida, J. Chem. Phys. **88**, 7410 (1988).
[16] A. Gilchrist, G. Hancock, R. Peverall, G. Richmond, G. A. D. Ritchie, and S. Taylor, J. Phys. Chem. A **112**, 4531 (2008).
[17] M. Dantus, M. H. M. Janssen, and A. H. Zewail, Chem. Phys. Lett. **181**, 281 (1991).
[18] M. H. M. Janssen, M. Dantus, H. Guo, and A. H. Zewail, Chem. Phys. Lett. **214**, 281 (1993).
[19] J. C. Owrutsky and A. P. Baronavski, Chem. Phys. Lett. **222**, 335 (1994).
[20] J. A. Syage, Chem. Phys. Lett. **212**, 124 (1993).
[21] P. G. Wang and L. D. Ziegler, J. Chem. Phys. **95**, 288 (1991).
[22] G. N. A. Van Veen, T. Baller, and A. E. de Vries, Chem. Phys. **97**, 179 (1985).
[23] R. E. Continetti, B. A. Balko, and Y. T. Lee, J. Chem. Phys. **89**, 3383 (1988).
[24] W. G. Roeterdink, A. M. Rijs, and M. H. M. Janssen, J. Am. Chem. Soc. **128**, 576 (2006).
[25] B. J. Sussman, D. Townsend, M. Y. Ivanov, and A. Stolow, Science **314**, 278 (2006).
[26] R. de Nalda, J. G. Izquierdo, J. Durá, and L. Bañares, J. Chem. Phys. **126**, 021101 (2007).
[27] R. de Nalda, J. Durá, A. García-Vela, J. González-Izquierdo, J. González-Vázquez, and L. Bañares, J. Chem. Phys. **128**, 244309 (2008).
[28] J. Durá, R. de Nalda, J. Álvarez, J. G. Izquierdo, G. A. Amaral, and L. Bañares, ChemPhysChem **9**, 1245 (2008).
[29] J. Durá, R. de Nalda, G. A. Amaral, and L. Bañares, J. Chem. Phys. **131**, 134311 (2009).
[30] K. L. Wells, G. Perriam, and V. G. Stavros, J. Chem. Phys. **130**, 074308 (2009).
[31] W. G. Roeterdink and M. H. M. Janssen, Chem. Phys. Lett. **345**, 72 (2001).
[32] W. G. Roeterdink and M. H. M. Janssen, Phys. Chem. Chem. Phys. **4**, 601 (2002).
[33] A. T. J. B. Eppink and D. H. Parker, Rev. Sci. Instrum. **68**, 3477 (1997).
[34] G. A. Garcia, L. Nahon, and I. Powis, Rev. Sci. Instrum. **75**, 4989 (2004).
[35] V. Loriot, L. Bañares, and R. de Nalda (unpublished).
[36] A. T. J. B. Eppink and D. H. Parker, J. Chem. Phys. **109**, 4758 (1998).
[37] W. P. Hess, R. Naaman, and S. R. Leone, J. Phys. Chem. **91**, 6085 (1987).
[38] R. N. Zare, *Angular Momentum. Understanding Spatial Aspects in Chemistry and Physics* (Wiley, New York, 1998).
[39] C. Jonah, J. Chem. Phys. **55**, 1915 (1971).
[40] S. Yang and R. Bersohn, J. Chem. Phys. **61**, 4400 (1974).